



PLA Films Incorporated with Chitosan and ZnO Nanoparticles for Application in Food Packaging

Flávia Z. Sanches^a , Kleper de O. Rocha^a , Carlos Henrique G. Martins^b ,
Lamartine L. de Melo^b, Aroldo G. Magdalena^{a*} 

^aUniversidade Estadual Paulista, Faculdade de Ciências, Departamento de Química, 17033-260, Bauru, SP, Brasil.

^bUniversidade Federal de Uberlândia, Instituto de Ciências Biomédicas, Departamento de Microbiologia, 38405-302, Uberlândia, MG, Brasil.

Received: June 11, 2024; Revised: August 02, 2024; Accepted: September 01, 2024

Biopolymers such as PLA, ZnO nanoparticles and chitosan are materials that have some properties in common, such as oxidizing action, antimicrobial activity, biocompatibility and formation of a mechanical barrier, which make them promising for application in food packaging, as they ensure safety in contact with food. In this study, the antibacterial activity of pure PLA films and those incorporating chitosan, ZnO nanoparticles and both was analyzed for four strains (two Gram-positive and two Gram-negative bacteria) by the agar diffusion method, aiming to verify the action of each substance and their combination. The characterization of ZnO NPs was performed by XRD, FTIR, Raman spectroscopy, UV-Vis, SEM and Zeta potential (ZP) methods. The results showed that the ZnO nanoparticles synthesized by the Pechinhi method, with calcination temperatures of 600 and 800°C, presented a predominant morphology of nanorods and nanospheres, according to SEM images, with high purity and crystallinity. The PLA-based films presented a rough structure, with small pores, and the incorporation of chitosan and ZnO NPs was effective, which was proven by the SEM/EDS technique. The results showed that the films incorporated with ZnO NPs presented inhibition for Gram-positive bacteria in the range of 12.5 to 14 mm.

Keywords: Zinc oxide, nanoparticles, chitosan, PLA films, food packaging, antimicrobial activity.

1. Introduction

The function of packaging is to protect and maintain the quality of products, mainly against external factors. However, to fulfill this function, toxic compounds derived from petroleum are often used, which can cause harm to the environment and human health. If packaging is not adequate, food may deteriorate due to the growth of microorganisms that can cause serious infectious diseases and food poisoning^{1,2}.

The most common packaging plastics are poly(ethylene), poly(ethylene terephthalate), poly(propylene), poly(vinyl chloride) and poly(styrene). As these materials are not biodegradable, they take hundreds or even thousands of years to decompose, contributing significantly to environmental pollution^{1,3,4}.

Aiming to reduce these impacts, research is being carried out focused on the development and promotion of the use of biopolymers, which offer benefits such as thermal stability, flexibility, barrier against gases and water, biodegradability, resistance to chemicals and biocompatibility³. These renewable biopolymers have stood out as sustainable solutions in several applications, including smart food packaging, biomedical and drug distribution, biomembranes, the automotive sector and industrial composting⁵.

Nanotechnology can help combat resistant bacteria through nanocomposites with antimicrobial properties. These compounds act on bacterial receptors through a complexation reaction, preventing their growth or division and, thus, preventing the spread of pathogens⁶. Zinc oxide nanoparticles are especially interesting due to this characteristic, offering great conservation potential. Therefore, to improve the quality of polymers used in food packaging, the incorporation of nanostructured zinc oxide in these matrices is a significant option, as it is effective as an antibacterial agent against several types of bacteria, both Gram-positive and Gram-negative^{7,8}.

Chitosan is a polysaccharide considered safe and sustainable by the United States Environmental Protection Agency, due to its notable advantages, such as non-toxicity, biodegradability, biocompatibility, antioxidant properties, and its natural production and regeneration, contrasting with petroleum-derived materials and coal. Because it is an abundant by-product, resulting from discarded fishing, and because it is renewable, it has a reduced cost, giving it significant economic and environmental relevance⁹⁻¹¹. Furthermore, this biopolymer has effective antimicrobial properties against Gram-positive and Gram-negative bacteria, as well as fungi and yeast. This makes it attractive for a

*e-mail: aroldo.magdalena@unesp.br

wide variety of applications in different sectors, both in its pure form and when incorporated into other polymers¹¹⁻¹⁴.

Poly (lactic acid), PLA, is a thermoplastic, biodegradable and biocompatible aliphatic polyester, which can be semi-crystalline or amorphous. It is of natural origin, composed of lactic acid molecules, obtained from renewable sources such as corn, cassava, sugar cane, beetroot, potatoes and other starchy vegetables¹⁵⁻¹⁷.

Among the main advantages of PLA biopolymer are: biodegradability, which can be decomposed by microorganisms under appropriate composting conditions; biocompatibility and biological absorption, making it safe for applications in the medical, dental, pharmaceutical and food industries; good mechanical properties of rigidity and resistance, enabling a wide range of uses; simple processing techniques such as extrusion, injection and thermal molding; thermal stability and transparency, useful for packaging that displays the product, such as food packaging, in addition to being dyeable for greater protection against UV rays; CO₂ consumption during synthesis; and low energy consumption in production. These characteristics make PLA a viable substitute for conventional petroleum-derived polymers, reducing environmental impact. The main disadvantage remains its high cost compared to conventional commercial plastics^{18,19}.

The Pechini method involves the formation of metal citrates by the interaction between a hydrocarboxylic acid and a metal cation. Then, a polyhydroxyalcohol, such as ethylene glycol, is added to the chelate, and the increase in temperature promotes esterification and polyesterification reactions until the formation of a polymeric resin. This resulting gel is calcined to remove the organic matter and obtain the desired metallic oxide, forming a homogeneous polyester with the cations distributed in its structure²⁰⁻²². This technique allows precise control of the stoichiometry of atoms and generates particles of high purity, homogeneity and surface area. However, due to the several steps involved, the process can be slow, complex and have high costs^{22,23}.

Considering the characteristics of these materials and compounds, this work aims to investigate the influence of the incorporation of chitosan and ZnO nanoparticles into the PLA polymer matrix, regarding antimicrobial properties in contact with strains of Gram-positive and Gram-negative bacteria, for application in food packaging.

2. Materials and Methods

The reagents used for the synthesis of ZnO nanoparticles were citric acid monohydrate (99-102%), zinc chloride (99%) and ethylene glycol (96%), all from the Dinâmica brand.

To prepare the films, PLA filaments, dichloromethane (ECIBRA – 99,8%), double-distilled glycerin (Dinâmica – 99,5%), chitosan (Sigma-Aldrich – 99,999%) and ZnO nanoparticles obtained by the Pechini method were used. PLA, from the Voolt 3D brand, used as a base polymer, was obtained in the form of filament for a 3D printer, in natural color (transparent).

2.1. Synthesis of ZnO nanoparticles

Zinc oxide nanoparticles were synthesized using the polymeric precursor method (Pechini), by mixing solutions of citric acid monohydrate and zinc chloride, in a molar ratio

of 3:1 (citric acid:metal cation)²⁴. The solutions were kept under constant stirring for 2 hours at 80°C. Then, ethylene glycol was added, at a ratio of 40/60 (%w/w) in relation to citric acid. The temperature was raised to 120°C, for total evaporation of the water and formation of the polymeric resin. For the pyrolysis stage, the material was subjected to heating in a muffle furnace, at a temperature of 400°C (heating rate of 10°C/min), for 3 hours, until the formation of polyester, in the form of a characteristic foam, colored dark and shiny, known as puff. The resulting polyester went through a deagglomeration process, until it reached a fine powder, which was separated into two porcelain boats. In the final stage, to obtain the ZnO NPs, calcination was carried out in a muffle furnace, for one of the samples at a temperature of 600°C and, for the other, at 800°C (heating rate of 10°C/min), for 3 hours.

2.1.1. X-Ray diffraction (XRD)

The diffractometer used was Rigaku, model RINT 2000, operated under conditions of 40kV and 150 mA, with CuK α radiation ($\lambda = 1.5406 \text{ \AA}$), scanning speed of 0.02° per minute, and interval (2 θ) of 10° to 80°, at a speed of 0.5° min⁻¹.

2.1.2. Fourier transform infrared spectroscopic (FTIR)

The spectrometer used to obtain the data was a Vertex 70, from Bruker Instruments, with ATR diamond and using potassium bromide (KBr) tablets, using the total reflectance method, with a scan from 4000 to 400 cm⁻¹.

2.1.3. Raman spectroscopy

Raman measurements, referring to the vibrational aspects of molecular groups, were carried out on a Metrohm Raman Spectrometer equipment, model i-Raman Plus 532H/USA, applying a wavelength of 532 nm and 100% laser level power, in a Raman shift range of 200 to 800 cm⁻¹. The resulting spectrum was obtained by fusing ten spectra, collected in 60 s each, totaling 6 min, for each of the ZnO NPs samples.

2.1.4. UV-Vis spectroscopy

For these measurements, the LAMBDA 1050 UV/Vis/NIR spectrometer from PerkinElmer was used, with 150 mm fitting spheres and dual Si and InGaAs detectors. The scanning range was fixed in the range of 250 to 1000 nm.

2.1.5. Scanning electron microscopy (SEM)

The ZnO NPs were subjected to scanning electron microscopy to evaluate their morphologies, using Zeiss equipment, model EVO LS-15.

2.1.6. Zeta potential

For zeta potentials measurements, the Zetasizer Nano ZS equipment from the company Malvern Instruments was used.

2.2. Preparation of PLA-based films incorporated with chitosan and ZnO NPs

PLA-based films were obtained by dissolving 200 mg of PLA in 5 ml of dichloromethane (DCM) for approximately 48 hours. The mixture was kept under constant stirring in a hood, at 1000 rpm, with the addition of 2 drops of glycerol, for 30 minutes. The solution was placed in a 7 cm diameter

petri dish and left in the hood to dry, at room temperature, for 24 hours, to eliminate the solvent. The incorporation of chitosan was carried out by adding 80 mg of the substance. To add the ZnO NPs, 10 mg was used, and the mixture of chitosan and ZnO NPs was used 80 and 10 mg, respectively.

2.2.1. Scanning electron microscopy (SEM) and Energy dispersive X-ray spectroscopy (EDX)

In the films, a scanning electron microscope (SEM) was used, which uses a field emission gun (FEG) as an electron source, coupled to an energy dispersive X-ray spectrometry (EDS) system, from the brand Jeol, model JSM IT500-HR.

2.2.2. Antibacterial activity: assay by the agar diffusion (AD) method

Bacterial cultures used in the present studies were obtained from the American Type Culture Collection (ATCC). Four microbial strains were tested: Gram-positive - *Staphylococcus aureus* (ATCC 6538) and *Bacillus cereus* (ATCC 14579), and Gram-negative - *Escherichia coli* (ATCC 25922) and *Salmonella enterica subsp. enterica* (ATCC 14028).

The antibacterial activity of the samples was determined by the agar diffusion (AD) method, using the disc technique against the test bacteria²⁵. Initially, the Mueller-Hinton agar (MHa) culture medium was prepared. After cooling to around 50 °C, a volume of 25 mL of the liquefied medium was transferred to sterile 15 × 90 mm diameter Petri dishes, until it reached a thickness of 4 mm. Using a sterile swab, the inoculum (1.5 × 10⁸ CFU/mL) was distributed evenly over the surface of the agar and left to stand at room temperature for 3 min. Disks from PLA and PLA incorporated with ZnO NPs, chitosan and the combination of these, were placed on the agar surface. After an interval of 15 min, the plates were incubated in a bacteriological oven at 36°C for 18 h. Chloramphenicol (30 µg) and imipenem (10 µg) discs were used as positive controls. Bacterial growth inhibition was determined as the diameter of the inhibition zones around the discs and were measured in millimeters using a millimeter ruler. All tests were performed in triplicate.

3. Results and Discussion

3.1. Synthesis of ZnO nanoparticles

The synthesis of ZnO NPs was carried out using the Pechini method, with citric acid and zinc chloride as precursors. After the metal citrate pyrolysis step, the sample was divided into two parts, one subjected to calcination at 600° and the other at 800°C, as specified in the characterization graphics below.

3.1.1. X-Ray diffraction (XRD)

The Figure 1 shows the X-ray diffraction patterns of ZnO NPs, obtained for the two calcination temperatures (600°C and 800°C), with zinc chloride as the precursor. The Bragg diffraction peaks are characteristic of the hexagonal structure, wurzite, for zinc oxide crystals.

By analyzing the diffractograms, it is possible to observe, for the two samples, well-defined peaks and the absence of additional impurity peaks, meaning that the zinc oxide nanoparticles, synthesized by Pechini, have high purity and crystallinity. The intensities were proportionally greater with

the increase in the calcination temperature, which is possible to verify through the elongation and narrowing of the peaks in the sample calcined at 800°C, compared to that subjected to calcination at 600°C.

The peaks at $2\theta = 31,77076^\circ$, $34,44688^\circ$, $36,26843^\circ$, $47,56715^\circ$, $56,61587^\circ$, $62,90208^\circ$, $65,96185^\circ$, $67,98429^\circ$ and $69,11140^\circ$, for the sample calcined at 600°C and $31,75711^\circ$, $34,43128^\circ$, $36,25133^\circ$, $47,55214^\circ$, $56,60258^\circ$, $62,89478^\circ$, $65,98518^\circ$, $67,97532^\circ$, $69,10466^\circ$ for calcined at 800°C were assigned to (100), (002), (101), (102), (110), (103), (200), (112) and (201), respectively, corresponding to the reflection planes of the hexagonal wurzite structure of ZnO²⁶.

3.1.2. Fourier transform infrared spectroscopic (FTIR)

FTIR was performed to detect the functional groups present in the ZnO NPs samples, in the range of 500 to 4000 cm⁻¹, as shown in Figure 2.

The two samples presented main absorption peaks in the same regions (496 cm⁻¹, 1224 cm⁻¹, 1383 cm⁻¹, 1729 cm⁻¹, 2366 cm⁻¹, 2930 cm⁻¹, 3092 cm⁻¹, 3463 cm⁻¹). The spectrum range between 400 and 500 cm⁻¹ is related to the vibrational

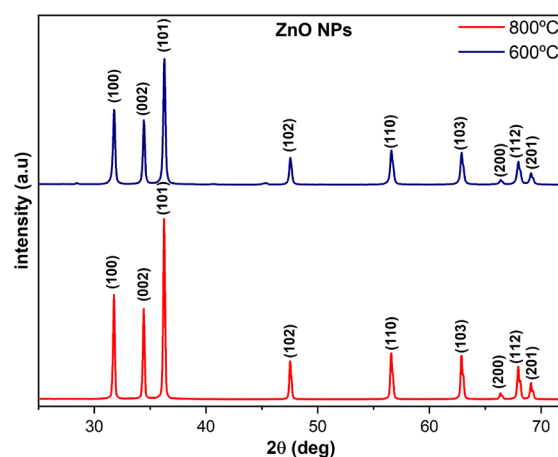


Figure 1. XRD patterns of ZnO NPs calcined at 600°C and 800°C.

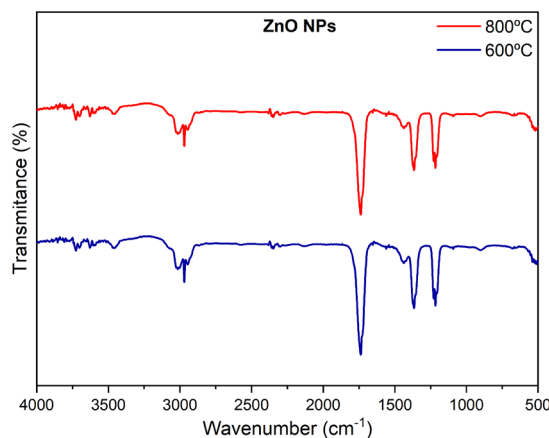


Figure 2. FTIR spectra of ZnO NPs calcined at 600°C and 800°C.

mode of metal-oxygen bonds. Thus, the sharp absorption peak at 495 cm^{-1} refers to the stretching of the Zn-O bond, confirming the formation of the substance²⁷.

The intense peak at 1224 cm^{-1} comprises a region related to the stretching vibration of the C-O single bond and the following peak, also of high intensity, at 1383 cm^{-1} , to the C-H stretching. The most intense peak in the sample, located at 1729 cm^{-1} , represents the stretching vibration of the carbonyl group (C=O). The region of discrete peaks at 2366 cm^{-1} can be related to the absorption of CO_2 , present in the atmosphere, from metallic cations. The peaks formed in the region around 3000 cm^{-1} have lower intensity and are characteristic of the C-H group. More discreet, the peak around 3463 cm^{-1} refers to the characteristic absorption of hydroxyl groups, it corresponds to the O-H stretching of the intramolecular hydrogen bond^{28,29}.

3.1.3. Raman spectroscopy

The graph in Figure 3 demonstrates, for both samples of ZnO NPs, that the main peak was formed at 438 cm^{-1} , which corresponds to the E_2 (high) mode, associated with the vibration of O, for the wurzite structure of ZnO, and which is related to the degree of crystallinity³⁰. These data corroborate the data obtained from FTIR for the formation of zinc oxide.

3.1.4. UV-Vis spectroscopy

From the observation spectra in the UV-Vis region, of ZnO NPs, shown in Figure 4, for both samples it is possible to note that the maximum observation occurred at a wavelength of 324 nm , in the UV region, a characteristic attributed to the electronic transition of ZnO, confirming the formation of the inorganic compound. In the visible area, the spectra show low absorption³¹. The ZnO NPs calcined at 800°C showed a higher absorption peak compared to 600°C .

It is possible to identify that the absorption values of ZnO NPs are high for lower wavelengths (less than 400 nm), but lower for longer wavelengths (above 450 nm). High absorbance in the shorter wavelength range is a property of opaque materials³². This may be since the analysis was carried out directly on the compacted powder, making it difficult for light to pass through.

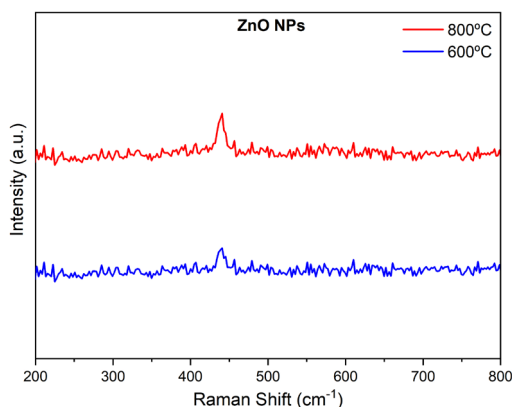


Figure 3. Raman spectrum of the ZnO NPs calcined at 600°C and 800°C .

3.1.5. Scanning electron microscopy (SEM)

As evidenced by the micrographs obtained in the SEM, shown in Figure 5, the calcination temperature had an influence on the final properties of the ZnO nanoparticles. In samples calcined at a temperature of 800°C , it appears that the crystallites had a larger average size compared to those treated at 600°C , also presenting a clearer crystalline structure. These observations confirm the results obtained in the X-ray diffractograms.

Regarding morphology, the nanoparticles appeared, for the most part, as nanorods or nanospheres, in some regions of agglomerates and with an average size about $25\text{--}150\text{ nm}$, for the sample calcined at 600°C and $40\text{--}200\text{ nm}$ for the one calcined at 800°C .

3.1.6. Zeta potential

For information regarding the stability of oxide nanoparticles of zinc synthesized, in colloidal suspension, due to their tendency to repel each other or if they aggregate, zeta potential measurements were carried out for both samples of ZnO NPs, depending on the pH of the solution, starting at pH 12 and adding HCl until pH 2, as shown in Figure 6 below.

Due to the differences in zeta potential between the samples, it appears that the calcination temperature interferes with the final surface structure and chemistry of ZnO NPs. The distinction between the values denotes the variation in the interactions between the particles and in the net density of the surface charge, which can also cause divergence in the properties of these nanoparticles.

With the increase in pH, the surface of the nanoparticles is negatively charged, due to the hydroxyl ions. As a result, the repulsion of the particles becomes more accentuated, increasing the colloidal property³³.

The ZnO NPs sample calcined at 800°C reached a higher zeta potential value, which means that it has greater colloidal stability. The SEM micrographs and XRD patterns for the ZnO NPs also demonstrated that the material calcined at a higher temperature presented a higher percentage of crystallinity

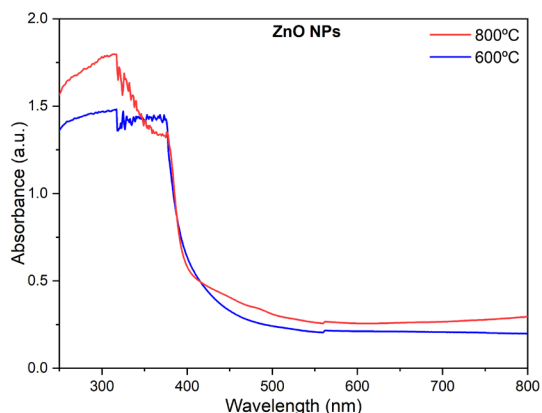


Figure 4. UV-Vis absorption spectra of ZnO NPs calcined at 600°C and 800°C .

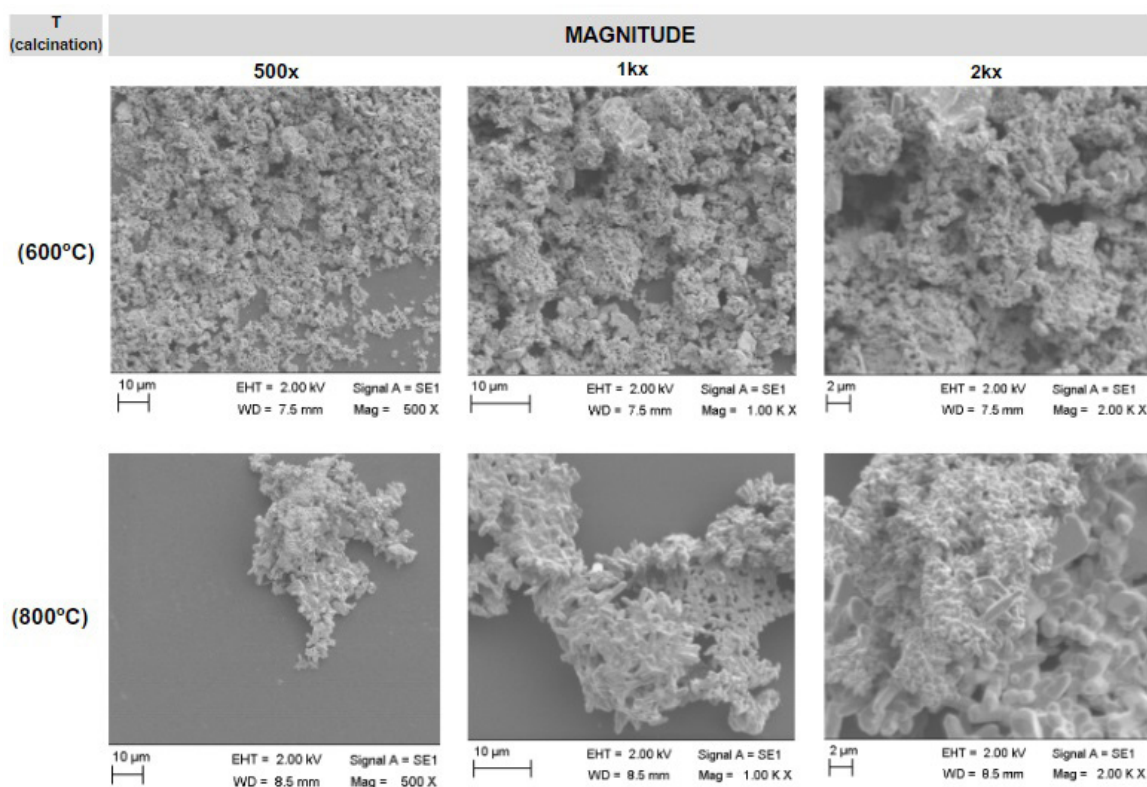


Figure 5. SEM images of ZnO NPs calcined at 600°C and 800°C, in magnitudes of 500x, 1 kx and 2kx.

and better-defined morphology, despite its larger size, in agreement with the zeta potential results.

The isoelectric point (pI), which corresponds to the balance between positive and negative charges, of the ZnO NPs samples was 4.06 for the sample calcined at 600°C and 3.35 for the one calcined at 800°C.

3.2. Preparation of PLA-based films incorporated with chitosan and ZnO NPs

Six PLA-based films obtained [PLA; PLA + ZnO (600°C); PLA + ZnO (800°C); PLA + CS; PLA + CS + ZnO (600°C); PLA + CS + ZnO (800°C)], are shown in Figure 7.

From image 7, it is possible to observe that the films have a slightly rough surface and that the ZnO NPs and chitosan are dispersed throughout the PLA, but there are some small deposition sites, as they are not soluble in dichloromethane, remaining suspended in the solution.

The addition of glycerin, as a plasticizing agent, made the PLA more resistant, making it possible to bend it without causing cracks or deformations.

3.2.1. Scanning electron microscopy (SEM) and Energy dispersive X-ray spectroscopy (EDS)

The cross-sectional morphology of PLA-based biofilms and the distribution of ZnO and chitosan (CS) nanocomposites were analyzed by scanning electron microscopy, and representative images are shown in Figure 8.

The poly (lactic acid) film, PLA, has a rough and heterogeneous texture, with the presence of cavities and

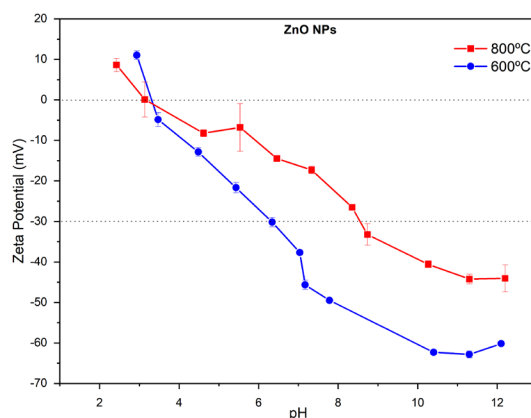


Figure 6. Zeta potentials of ZnO NPs calcined at 600°C and 800°C, measured as a function of pH.

pores throughout the structure being identified, but without cracks or fractures. The addition of glycerin, as a plasticizing agent, can be a significant factor in obtaining the final morphology, as when it penetrates the molecular structure, it causes a reduction in the attractive forces of the polymer chains, which also leads to increased flexibility, making the polymer more flexible and resistant to breakage. Another factor that can also generate these changes is the drying process, in which the evaporation of the solvent can create empty spaces, causing these holes³⁴.

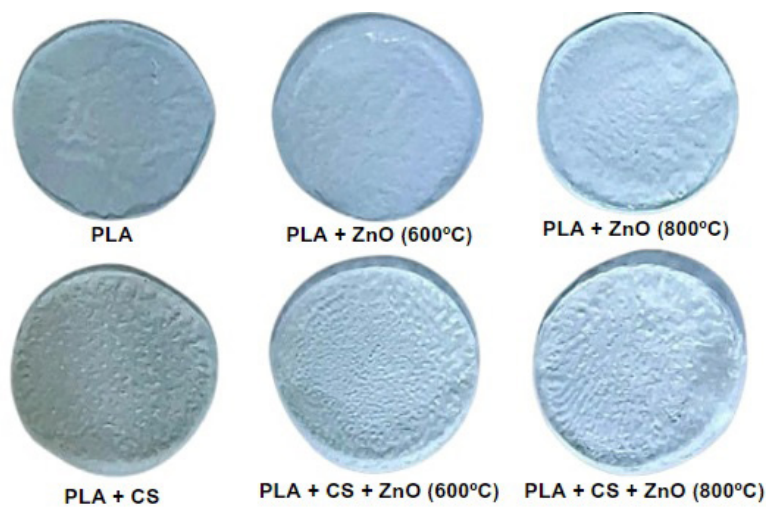


Figure 7. PLA, PLA+ZnO (600°C and 800°C), PLA+CS, and PLA+CS+ZnO (600°C and 800°C) films.

FILMS	MAGNITUDE			
	5.000x	10.000x	25.000x	50.000x
PLA				
PLA + ZnO (600°C)				
PLA + ZnO (800°C)				
PLA + CS				
PLA + CS + ZnO (600°C)				
PLA + CS + ZnO (800°C)				

Figure 8. Micrographs obtained by SEM of PLA, PLA+ZnO (600°C and 800°C), PLA+CS, and PLA+CS+ZnO (600°C and 800°C) films.

When incorporating ZnO NPs into the biopolymer, the nanoparticles appear as nanorods or nanospheres, in a more pronounced shape, in brighter areas. They also had a homogeneous distribution throughout the polymer matrix, highlighting some regions with association of small clusters. In nanocomposite films, the existence of a good dispersion of inorganic filler, through the polymer matrix, can result in improvements in the physical properties of the material³⁴.

Although the dispersion of chitosan directly in the PLA film is visible, it is not possible to distinguish the materials in the SEM images, since the addition of CS did not cause changes in the morphology of the biopolymer. However, through EDS analysis, it was possible to identify the chitosan particles, as indicated by the arrows in Figure 9.

The films that had the two substances added, ZnO and chitosan, generated irregular morphologies, but with good

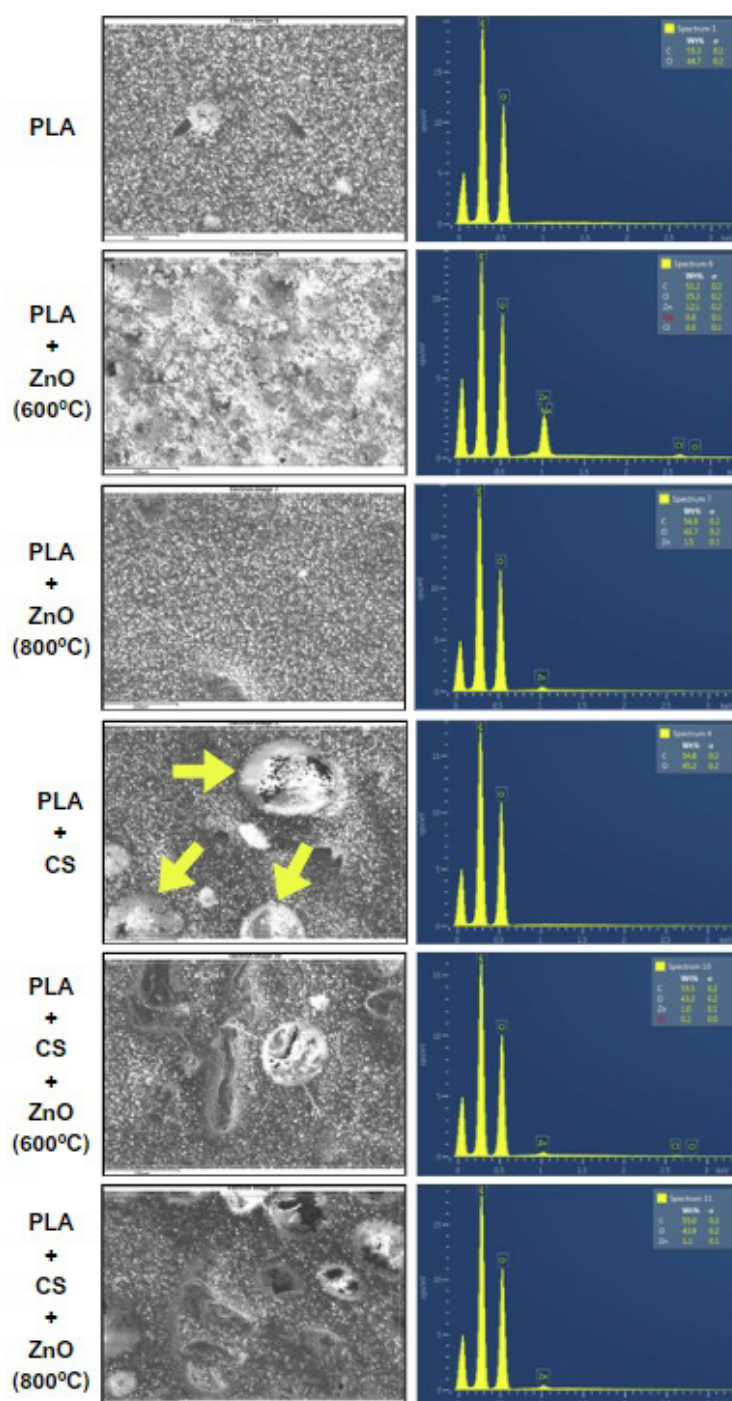


Figure 9. EDS spectra of PLA, PLA+ZnO (600°C and 800°C), PLA+CS, and PLA+CS+ZnO (600°C and 800°C) films.

Table 1. Antibacterial activity by agar diffusion (AD) method.

	Agar Diffusion (AD) Method – Inhibition halos (diameters in mm) – Mean ± Standard deviation							
	PLA	PLA + ZnO (600°C)	PLA + ZnO (800°C)	PLA + Chitosan	PLA + Chitosan + ZnO (600°C)	PLA + Chitosan + ZnO (800°C)	Chloramphenicol	Imipenem
Escherichia coli ATCC 25922	0.0 ± 0.0	0.0 ± 0.0	0.0 ± 0.0	0.0 ± 0.0	0.0 ± 0.0	0.0 ± 0.0	29.0 ± 0.0	21.6 ± 0.5
Salmonella enterica ATCC 14028	0.0 ± 0.0	0.0 ± 0.0	0.0 ± 0.0	0.0 ± 0.0	0.0 ± 0.0	0.0 ± 0.0	24.7 ± 0.5	30.3 ± 0.5
Bacillus cereus ATCC 14579	0.0 ± 0.0	14.0 ± 0.0	13.3 ± 0.5	0.0 ± 0.0	14.0 ± 0.0	13.7 ± 0.5	27.3 ± 2.5	43.7 ± 1.9
Staphylococcus aureus ATCC 6538	0.0 ± 0.0	12.8 ± 0.8	12.5 ± 1.1	0.0 ± 0.0	12.6 ± 0.5	13.2 ± 1.2	26.0 ± 0.0	45.7 ± 0.5

dispersion. Even in a smaller proportion, ZnO NPs appear predominantly in the micrographs, and with good incorporation into PLA, in mostly nanorod structures, standing out in relation to chitosan.

Energy dispersive X-ray spectroscopy (EDS) was used to identify the elements that make up the samples and analyze the presence of possible contaminants. The EDS patterns are represented by Figure 9, with the captured X-ray images.

The percentage by weight of the chemical composition, identified in the samples using the EDS technique, revealed that carbon and oxygen are the most abundant elements in all the films analyzed. Considering that hydrogen hardly produces X-rays, due to its electronic structure and energetic properties, and is rarely identified in EDS, the results are consistent with the materials used. The base of the films is the polymer PLA ($C_3H_4O_2$)_n, composed of lactic acid units, with 50% weight percentage carbon and about 44% oxygen.

In all films that had the incorporation of ZnO NPs, zinc was identified, however in the PLA + ZnO (600°C) sample an indicator of the presence of sodium (Na) also appeared, in red, which could be contamination in the handling of the product, material or spectral failure (interferences or overlaps).

Chitosan has the chemical formula ($C_6H_{11}NO_4$)_n, and is therefore also represented mainly by the elements C and O, since nitrogen also requires special conditions for identification by EDS, presenting low sensitivity to the technique. Another significant factor, presented by EDS, is that the films that had incorporated ZnO NPs calcined at 600°C, both alone and together with chitosan, showed signs of the element chlorine (Cl), originating from the $ZnCl_2$ precursor, demonstrating that this temperature was not sufficient to eliminate it. With the samples involving ZnO NPs calcined at 800°C, the presence of intermediate synthesis compounds or other contaminants was not identified.

3.2.2. Antibacterial activity: assay by the agar diffusion (AD) method

The results obtained for PLA-based biofilms with the addition of ZnO NPs and chitosan, after carrying out the agar disk diffusion tests, demonstrated that there was inhibition in the biofilm tests that had the incorporation of ZnO nanoparticles, both calcined and 600°C and 800°C, due to the appearance of inhibition halos around the discs of deposited biofilms, for Gram-positive bacteria (*Staphylococcus aureus* and *Bacillus cereus*). For Gram-negative bacteria, no growth inhibition zone was formed, proving ineffective

as an antibacterial for *Escherichia coli* and *Salmonella enterica*. The structure of bacterial cell membranes may be related to the divergence in these responses, as Gram-positive bacteria are composed of teichoic acids and layers of peptidoglycan, a substance responsible for the rigidity of the cell wall, while Gram-negative bacteria have one or a few layers of peptidoglycan in addition to another outer membrane composed of lipopolysaccharides (LPS) and proteins, which makes it more resistant³⁵.

In the samples that contained only PLA and chitosan incorporated into the biopolymer, no significant inhibitory areas were detected for any of the types of bacteria, Gram-negative and Gram-positive. In PLA discs that had chitosan and ZnO NPs integrated into the polymeric matrix, the response was like those in which only ZnO NPs were added, demonstrating that chitosan did not influence the antimicrobial property.

According to the literature, chitosan has high antimicrobial properties. However, when incorporated into PLA, the antibacterial efficacy of chitosan may be affected due to some factors, such as the proportion of chitosan added to the polymer matrix, the processing method and the interaction of these materials³⁶⁻³⁸. Another hypothesis regarding the inactivation of the antimicrobial action of chitosan may be the occurrence of encapsulation of these particles by PLA, making it difficult for them to encounter bacteria.

The test was also applied, for comparative purposes, to two samples of antibiotics, chloramphenicol and imipenem, drugs aimed at treating bacterial infections, that is, with great antimicrobial potential, as shown in Table 1.

4. Conclusions

The synthesis of ZnO NPs using the Pechini method proved to be effective in obtaining a material with high crystallinity and purity, with a predominant form of nanorods. Through analysis, it was demonstrated that calcination temperatures are important factors in the product obtained, interfering in some properties and structural characteristics. The materials subjected to a temperature of 800°C showed greater crystallinity and diameter, compared to those calcined at 600°C, which resulted in smaller crystallites, but slightly less crystalline.

PLA-based biofilms exhibited a microstructure with roughness and the presence of small pores, but flexible and resistant.

The incorporation of ZnO NPs and chitosan into the PLA polymer matrix was carried out with the aim of offering antimicrobial properties, which were tested by the agar disk diffusion method. The results confirmed the antimicrobial activity of the discs that had the addition of ZnO NPs, for Gram-positive bacteria (*Staphylococcus aureus* and *Bacillus cereus*), through the inhibition halo formed, with no significant distinction between the applied calcination temperatures (600 and 800°C). Therefore, the size of the nanoparticles was not a relevant factor in the biocidal action. Efficiency has not been proven for more resistant Gram-negative bacteria. Chitosan did not demonstrate antimicrobial potential to any of the types of bacteria.

Considering the characteristics presented, the aggregation of ZnO NPs to biopolymers shows promise, as they are safe for health, easily inserted (by simple and economical methods), and improve mechanical and antimicrobial properties. This makes it a significant option in the area of food packaging, as it is capable of extending its shelf life, as well as helping to prevent contamination.

5. Acknowledgments

The authors would like to thank POSMAT/UNESP and FAPESP (process: 2013/07296-2).

6. References

- Kraśniewska K, Galus S, Gniewosz M. Biopolymers-based materials containing silver nanoparticles as active packaging for food applications—A review. *Int J Mol Sci*. 2020;21(3):698.
- Wrońska N, Katir N, Milowska K, Hammi N, Nowak M, Kedzierska M, et al. Antimicrobial effect of chitosan films on food spoilage bacteria. *Int J Mol Sci*. 2021;22(11):5839.
- Gabor D, Tita O. Biopolymers used in food packaging: a review. *Acta Univ Cibiniensis Ser E Food Technol*. 2012;XVI(2)
- Porta R, Sabbah M, Di Piero P. Biopolymers as food packaging materials. *Int J Mol Sci*. 2020;21(14):4942.
- Moustafa H, Youssef AM, Darwish NA, Abou-Kandil AI. Eco-friendly polymer composites for green packaging: future vision and challenges. *Compos, Part B Eng*. 2019;172:16-25.
- Agarwal H, Menon S, Kumar SV, Rajeshkumar S. Mechanistic study on antibacterial action of zinc oxide nanoparticles synthesized using green route. *Chem Biol Interact*. 2018;286:60-70.
- Espitia PJP, Soares NFF, Coimbra JSR, Andrade NJ, Cruz RS, Medeiros EAA. Zinc oxide nanoparticles: Synthesis, antimicrobial activity and food packaging applications. *Food Bioprocess Technol*. 2012;5(5):1447-64.
- Mendes CR, Dilarri G, Forsan CF, Sapata VMR, Lopes PRM, Moraes PB, et al. Antibacterial action and target mechanisms of zinc oxide nanoparticles against bacterial pathogens. *Sci Rep*. 2022;12(1)
- Azevedo VVC, Chaves AS, Bezerra DC, Fook MVL, Costa ACFM. Quitina e Quitosana: aplicações como biomateriais. *Revista Eletrônica de Materiais e Processos*. 2007;2(3):27-34.
- Li Q, Dunn ET, Grandmaison EW, Goosen MFA. *Applications of Chitin and Chitosan*. Boca Raton: CRC Press; 1996.
- Poznanski P, Hameed A, Orczyk W. Chitosan and chitosan nanoparticles: parameters enhancing antifungal activity. *Molecules*. 2023;28(7):2996.
- Kong M, Chen XG, Xing K, Park HJ. Antimicrobial properties of chitosan and mode of action: A state of the art review. *Int J Food Microbiol*. 2010;144(1):51-63.
- Macedo JB, Sanfelice RC, Mercante LA, Santos DM, Habitzreuter F, Campana-Filho SP. Atividade antimicrobiana de quitosanas e seus derivados: influência das características estruturais. *Quim Nova*. 2022;45(6):690-704.
- Meng W, Sun H, Mu T, Garcia-Vaquero M. Pickering emulsions with chitosan and macroalgal polyphenols stabilized by layer-by-layer electrostatic deposition. *Carbohydr Polym*. 2023;300(120256):120256.
- Brito GF, Agrawal P, Araújo EM, Melo TJA. Biopolímeros, Polímeros Biodegradáveis e Polímeros Verdes. *Revista Eletrônica de Materiais e Processos*. 2011;6(2):127-39.
- Garlotta D. A Literature Review of Poly(lactic acid). *J Polym Environ*. 2001;9(2):63-84.
- Hoseinnejad M, Jafari SM, Katouzian I. Inorganic and metal nanoparticles and their antimicrobial activity in food packaging applications. *Crit Rev Microbiol*. 2018;44(2):161-81.
- Fathima PE, Panda SK, Ashraf PM, Varghese TO, Bindu J. Polylactic acid/chitosan films for packaging of Indian white prawn (*Fenneropenaeus indicus*). *Int J Biol Macromol*. 2018;117:1002-10.
- Wan L, Zhou S, Zhang Y. Parallel advances in improving mechanical properties and accelerating degradation to polylactic acid. *Int J Biol Macromol*. 2019;125:1093-102.
- Costa ACF, Ramalho MAF, Neiva LSS, Alves-S Jr, Kiminami RHGA. Avaliação do tamanho da partícula do ZnO obtido pelo método Pechini. *Revista Eletrônica de Materiais e Processos*. 2007;2(3):14-9.
- Dimesso L. Pechini processes: an alternate approach of the sol-gel method, preparation, properties, and applications. In: Klein L, Aparicio M, Jitianu A. (Eds.). *Handbook of sol-gel science and technology*. Cham: Springer International Publishing; 2016. p. 1-22.
- Pechini MP. Method of preparing lead and alkaline earth titanates and nionates and coating method using the same form a capacitor. United States Patent No.3,330,697, July 11, 1967.
- Rocha RA, Muccillo ENS. Efeito da temperatura de calcinação e do teor de dopante nas propriedades físicas da céria-gadolínia preparada pela complexação de cátions com ácido cítrico. *Cerâmica*. 2001;47(304):219-24.
- Bonifácio MAR, Lira HR, Neiva LS, Kiminami RHGA, Gama L. Nanoparticles of ZnO doped with Mn: structural and morphological characteristics. *Mater Res*. 2017;20(4):1044-9.
- CLSI: Clinical and Laboratory Standards Institute. Performance standards for antimicrobial disk susceptibility tests, approved standard: CLSI M02-Ed13. 13th ed. Wayne, PA: Clinical and Laboratory Standards Institute; 2018.
- Devaraj R, Karthikeyan K, Jeyasubramanian K. Synthesis and properties of ZnO nanorods by modified Pechini process. *Appl Nanosci*. 2013;3(1):37-40.
- Srivastava V, Gusain D, Sharma YC. Synthesis, characterization and application of zinc oxide nanoparticles (n-ZnO). *Ceram Int*. 2013;39(8):9803-8.
- Yusof HM, Rahman AN, Mohamad R, Zaidan UH, Samsudin AA. Biosynthesis of zinc oxide nanoparticles by cell-biomass and supernatant of *Lactobacillus plantarum* TA4 and its antibacterial and biocompatibility properties. *Sci Rep*. 2020;10(1):1-13.
- Selva Esakki E, Vivek P, Devi LR, Sarathi R, Sheeba NL, Sundar SM. Influence on electrochemical impedance and photovoltaic performance of natural DSSC using Terminalia catappa based on Mg-doped ZnO photoanode. *J Indian Chem Soc*. 2022;99(12):100756.
- Sharma A, Singh BP, Dhar S, Gondorf A, Spasova M. Effect of surface groups on the luminescence property of ZnO nanoparticles synthesized by sol-gel route. *Surf Sci*. 2012;606(3-4):L13-7.
- Chikkanna MM, Neelagund SE, Rajashekarappa KK. Green synthesis of Zinc oxide nanoparticles (ZnO NPs) and their biological activity. *SN Applied Sciences*. 2019;1(1):117.
- Shabannia R, Hassan HA. Characteristics of photoconductive UV photodetector based on ZnO nanorods grown on polyethylene

- naphthalate substrate by chemical bath deposition method. *Electron Mater Lett*. 2014;10(4):837-43.
33. Leandro-Silva E, Silveira MLDC, Pipi ARF, Piacenti-Silva M, Magdalena AG. Metal removal using Fe₃O₄-Chitosan nanoparticles for environmental applications. *Revista Virtual de Química*. 2024;16(1):98-105.
 34. Kim YH, Priyadarshi R, Kim JW, Kim J, Alekseev DG, Rhim JW. 3D-printed pectin/carboxymethyl cellulose/ZnO bio-inks: comparative analysis with the solution casting method. *Polymers (Basel)*. 2022;14(21):4711.
 35. Firoozabadi FD, Saadatabadi AR, Asefnejad A. In vitro studies and evaluation of antibacterial properties of biodegradable bone joints based on PLA/PCL/HA. *Journal of Clinical Research in Paramedical Sciences*. 2022;11(1)
 36. Rahaman H, Gafur A, Hasanuzzaman, Habib R, Dhar SA, Hosen S. Poly(lactic acid)/chitosan blends: preparation, characterization and antibacterial activity. In: *Proceedings of the 1st International Conference on Engineering Materials and Metallurgical Engineering (ICEMME)*. Dhaka: ICEMME; 2016. p. 50-57
 37. Rihayat T, Hadi AE, Aidy N, Safitri A, Siregar JP, Cionita T, et al. Biodegradation of Polylactic Acid-based bio composites reinforced with chitosan and essential oils as anti-microbial material for food packaging. *Polymers (Basel)*. 2021;13(22):4019.
 38. Salazar R, Salas-Gomez V, Alvarado AA, Baykara H. Preparation, characterization and evaluation of antibacterial properties of polylactide-polyethylene glycol-chitosan active composite films. *Polymers (Basel)*. 2022;14(11):2266.